

LETTER • OPEN ACCESS

## Offshore fresh groundwater in coastal unconsolidated sediment systems as a potential fresh water source in the 21st century

To cite this article: Daniel Zamrsky *et al* 2022 *Environ. Res. Lett.* **17** 014021

View the [article online](#) for updates and enhancements.

You may also like

- [Analysis and Recommendations of Sand Consolidation Methods to Limit Sand Production in Gas Wells](#)  
Dmitry Tananykhin, Pavel Tsvetkov and Vladislav Kamoza
- [Analytical solutions for flow of horizontal well in compressible, three-dimensional unconsolidated formations](#)  
Yu-Long Zhao, Lie-Hui Zhang, Jun Chen et al.
- [Impact of head models in N170 component source imaging: results in control subjects and ADHD patients](#)  
L Beltrachini, A Blenkmann, N von Ellenrieder et al.

ENVIRONMENTAL RESEARCH  
LETTERS

## LETTER

## Offshore fresh groundwater in coastal unconsolidated sediment systems as a potential fresh water source in the 21st century

## OPEN ACCESS

RECEIVED  
20 August 2021REVISED  
1 December 2021ACCEPTED FOR PUBLICATION  
6 December 2021PUBLISHED  
30 December 2021

Original content from  
this work may be used  
under the terms of the  
[Creative Commons  
Attribution 4.0 licence](#).

Any further distribution  
of this work must  
maintain attribution to  
the author(s) and the title  
of the work, journal  
citation and DOI.

Daniel Zamrsky<sup>1,\*</sup> , Gualbert H P Oude Essink<sup>1,2</sup> , Edwin H Sutanudjaja<sup>1</sup>, L P H (Rens) van Beek<sup>1</sup>  
and Marc F P Bierkens<sup>1,2</sup> <sup>1</sup> Department of Physical Geography, Utrecht University, Utrecht, The Netherlands<sup>2</sup> Deltares, Delft, The Netherlands

\* Author to whom any correspondence should be addressed.

E-mail: [d.zamrsky@uu.nl](mailto:d.zamrsky@uu.nl)**Keywords:** unconsolidated, sediment, offshore fresh groundwater, SEAWAT modelsSupplementary material for this article is available [online](#)**Abstract**

Coastal areas worldwide are often densely populated and host regional agricultural and industrial hubs. Strict water quality requirements for agricultural, industrial and domestic use are regularly not satisfied by surface waters in coastal areas and consequently lead to over-exploitation of local fresh groundwater resources. Additional pressure by both climate change and population growth further intensifies the upcoming water stress and raise the urgency to search for new fresh water sources. In recent years, offshore fresh groundwater (OFG) reserves have been identified as such a potential water source. In this study, we quantify, for the first time, the global volume of OFG in unconsolidated coastal aquifers using numerical groundwater models. Our results confirm previously reported widespread presence of OFG along the global coastline. Furthermore, we find that these reserves are likely non-renewable resources mostly deposited during glacial periods when sea levels were substantially lower compared to current sea level. We estimate the total OFG volume in unconsolidated coastal aquifers to be approximately  $1.06 \pm 0.2$  million km<sup>3</sup>, which is roughly three times more than estimated previously and about 10% of all terrestrial fresh groundwater. With extensive active and inactive offshore oil pumping present in areas of large OFG reserves, they could be considered for temporary fresh groundwater exploration as part of a transition to sustainable water use in coastal areas on the long run.

**1. Introduction**

During recent decades, coastal communities settled along the global coastline have been subject to rising fresh water stress caused by both natural (Oude Essink *et al* 2010, Faneca Sánchez *et al* 2012, Rasmussen *et al* 2013, Yu *et al* 2016, Yang *et al* 2018) and anthropogenic (Syvitski *et al* 2009, Yamanaka *et al* 2011, Giosan *et al* 2014, van Camp *et al* 2014, Tessler *et al* 2015, Minderhoud *et al* 2017) causes. It might appear that the onshore and offshore zones of the global coast are geographically clearly defined as sea level stayed relatively constant (Lambeck *et al* 2014) throughout human recorded history. However, this coastal boundary is in reality rather dynamic when considering a larger geologic time scale. Before around 20 000 years ago,

during the Last Glacial Maximum, global mean sea level was more than 120 m lower than current sea level. As a result, extensive continental shelf areas, nowadays submerged under shallow seas, were exposed to terrestrial conditions for tens of thousands of years and hosted an environment full of rivers and fresh water lakes (Head and Gibbard 2005). Under such circumstances, vast fresh groundwater volumes developed through precipitation (i.e. meteoric water), via increased fresh groundwater inflow from inland due to greater groundwater head gradient and through extensive fresh surface water systems covering the current continental shelf areas.

Following the first global overview of offshore fresh groundwater (OFG) (Post *et al* 2013), which is based on numerous case studies since 1979 (Hathaway *et al* 1979), several regional scale studies

(Levi *et al* 2018, Morgan *et al* 2018, Gustafson *et al* 2019, Thomas *et al* 2019) have been conducted in recent years. It is important to mention that some other studies (Micallef *et al* 2020, 2021) define OFG as offshore freshened groundwater that also includes brackish levels of salinity; in our study OFG represents offshore fresh groundwater ( $<1 \text{ g l}^{-1}$  TDS (total dissolved solids)). It has been documented that OFG can be found tens or even hundreds of kilometers offshore while reaching depths of up to several kilometers. One of the most thoroughly studied and documented OFG occurrence is in the continental shelf off the New Jersey coast (Meisler *et al* 1984, Gustafson *et al* 2019, Thomas *et al* 2019). An extensive data acquisition of both geological and geophysical data was combined with numerical groundwater flow modelling (Gustafson *et al* 2019, Thomas *et al* 2019) to quantify the OFG volume stored in the porous unconsolidated sediments deposited at the continental shelf. OFG can also be stored in fractured karstic rocks as has been documented in e.g. Western and South-eastern Australia (Varma and Michael 2011, Morgan *et al* 2018). The abovementioned studies show that OFG is often preserved under low permeable geological layers that limit vertical seawater infiltration. These complex heterogeneous geological systems are found in both unconsolidated and karstic systems, stressing the need for a variety of geological information sources to successfully reconstruct regional offshore groundwater conditions. In our study, we combine global thickness estimates (Zamrsky *et al* 2018) and geological heterogeneity assessments (Zamrsky *et al* 2020) of unconsolidated sediment systems with variable-density groundwater flow and coupled salt transport modelling to estimate OFG volumes of the global coast (see section 2 and supporting information (SI) figure 1 (available online at [stacks.iop.org/ERL/17/014021/mmedia](https://stacks.iop.org/ERL/17/014021/mmedia))). Our study is solely focused on unconsolidated sediment systems, due to the lack of globally available data and the high variation in local characteristics of karstic systems (Chen *et al* 2017) (e.g. their complex conduit networks). Thus, when referring to global OFG volumes we refer to those in unconsolidated coastal aquifers only.

These regional geological scenarios, alongside other hydrogeological parameters (elevation, groundwater recharge estimation), are used for quantifying regional OFG volumes and their uncertainty by means of cross-sectional 2D variable-density groundwater flow and coupled salt transport models (called 'groundwater models' hereafter; SI figure 3). The temporal resolution of our numerical models covers the sea level fluctuation over one full glacial-interglacial cycle (Grant *et al* 2012) (approximately 125 000 years). This allows us to simulate past fresh water infiltration into the aquifers and aquitards that make up the present-day continental shelves during sea level low stands, and the subsequent salinization

of fresh groundwater resources, or their preservation under less permeable clay deposits, during fast rising sea levels in the past 20 000 years (Lambeck *et al* 2014). Herein, we measure salinity as total dissolved solids ( $\text{g l}^{-1}$  TDS) with fresh groundwater threshold defined as  $1 \text{ g l}^{-1}$  TDS which is the upper limit considered acceptable to consumers, as defined by World Health Organization (2017). Further details are provided in the section 2 and the SI.

## 2. Methods

### 2.1. Regional representative coastal groundwater flow models

The global analysis approach in our study consists of dividing the global coast into regions with similar geological characteristics. This is based on the assumption that coastal zones act as sinks for sediments transported downstream by rivers. These unconsolidated sediments are deposited both onshore, forming so called coastal plains, and offshore, on top of the continental shelves. Splitting up the global coast is based on the COSCAT (Meybeck *et al* 2006) and MARCAT (Laruelle *et al* 2013) datasets that define the sediment sources and sinks respectively. Combining these two datasets allows us to define regions with similar geological characteristics and to implement the geological heterogeneity quantification and geological scenario algorithm to create regional groundwater representations in each individual region. We refer to previous research (Zamrsky *et al* 2020) for an elaborate description of this approach and provide a summary below.

In estimating OFG volumes, we divided the global coastline into 116 regions (COSCAT regions) linking inland sediment sources with coastal and offshore sediment sinks (Meybeck *et al* 2006, Laruelle *et al* 2013) to capture global geological differences. The division into 116 regions is based on the number of coastal COSCAT regions that contain coastal unconsolidated sediment aquifer-aquitard systems (Zamrsky *et al* 2020). Equidistant cross-sectional profiles perpendicular to the coastline are constructed in areas formed by unconsolidated sediments in each COSCAT region (SI figure 1(A)). These regions are outlined by using the Global Lithological Map (Hartmann and Moosdorf 2012) dataset describing surficial lithology on global scale. Various attribute values are extracted along each profile (i.e. topography (Weatherall *et al* 2015), bathymetry (Weatherall *et al* 2015), long term average actual evapotranspiration and precipitation (NTSG 2019), hydraulic conductivity (Gleeson *et al* 2014, Huscroft *et al* 2018), soil type (Montzka *et al* 2017) and thickness (Hengl *et al* 2014), water table depth (Fan *et al* 2013). Two coastal types are defined to take into account variations in topography and aquifer-aquitard system thickness. A 'delta' coastal type represents major deltaic systems (Tessler *et al* 2015)

which likely have a wider (and thicker) coastal plain and continental shelf than the other profiles in the same region due to higher sediment input transported by rivers. Coastal types that are located in non-deltaic regions are named ‘coastal stretch’ and represent the vast majority of coastal profiles considered in this study.

An average representative profile (ARP) is built for each coastal type/COSCAT region combination which delineates its average geometrical conditions (topography and sediment depth) (SI figure 1(B)). To this end, all topography and bathymetry profiles are combined first to create the upper ARPs boundary. Next, after defining the current coastline position, an average thickness of the unconsolidated groundwater system is calculated and set as depth of the ARP at the coastline. In the following step, the continental shelf edge is identified as well as the foot of continental slope using a bathymetry slope algorithm (Wu *et al* 2017), which requires elevation as main input. When the foot of continental slope is successfully estimated, the bottom boundary of the offshore domain is defined as a line between the unconsolidated groundwater system depth at coastline and the foot of continental slope. If the continental slope is not found (e.g. in case of shallow bathymetry stretching far offshore), the offshore extent of the ARP is limited to 200 km and the bottom boundary is set to follow the average bathymetry slope of the offshore domain. The maximum offshore extent of 200 km is based on previous studies dealing with coastal and offshore groundwater models (Michael *et al* 2016, Zamrsky *et al* 2018, 2020).

A set of variable-density groundwater flow and coupled salt transport models (referred to as ‘groundwater models’ hereafter) is built for each ARP (coastal type/COSCAT region combination) (SI figures 1(c) and 3) in order to estimate groundwater salinity profiles. The SEAWAT code (Langevin and Guo 2006) is used to build the groundwater models. A total of 24 groundwater models with different geological setups (scenarios) are built for each ARP in order to capture unknown geological heterogeneity of the onshore and offshore sedimentary deposits (SI figure 2). This leads to a total number of 2784 groundwater models (116 ARP regions  $\times$  24 geological scenarios). The number of geological scenarios corresponds to the number of geological parameter combinations that outline regional geological heterogeneity (Zamrsky *et al* 2020 and SI text 1). In these geological scenarios, which are informed by regional sediment influx and size upstream from the coast and by preservation potential of coastal sediments, we vary the thickness and number of low permeable (aquitards) and highly permeable (aquifers) sediment layers and their shape in the offshore domain (Zamrsky *et al* 2020). The variation in number of aquitard and aquifer layer combinations is based on literature review of unconsolidated sediment aquifer-aquitard systems worldwide

(Zamrsky *et al* 2020) and varies between two and five aquitard-aquifer layer combinations. The thickness of individual aquitard and aquifer layers is randomly assigned while the ratio of total aquifer and aquitard thickness matches an estimated regional sediment type fraction (called ‘sand/mud’ ratio in Zamrsky *et al* (2020)). Between the 24 geological scenarios, the number of aquitard-aquifer layers, the thicknesses of aquifers and aquitards, aquifer permeability, aquitard leakiness and the thickness of the offshore capping clay layer are varied randomly. This approach is based on previous research (Zamrsky *et al* 2018, 2020) and further technical information is provided in SI texts 1 and 2.

## 2.2. OFG volume estimation

The groundwater salinity profiles of each simulation are aggregated for all ARPs’ 24 groundwater models based on the associated 24 geological scenarios, see SI figure 1(C). The mean groundwater salinity concentration value is then calculated for each groundwater model cell resulting in a mean groundwater salinity profile for each time step throughout the whole simulation duration. A threshold of 1 g l<sup>-1</sup> TDS is chosen as a boundary between fresh and brackish water which is in line with previous studies (Post *et al* 2013). The OFG volumes estimated for all ARP groundwater models for the same COSCAT region are aggregated to calculate the total OFG volumes  $V_{\text{total}}$  for the COSCAT region, see equation (1):

$$V_{\text{total}} = L_{\text{off}} \times D_{\text{shelf}} \times L_{\text{coast}} \times \frac{\text{FGF}_{\text{mean}}}{100} \times p \quad (1)$$

where  $L_{\text{off}}$  stands for modelled offshore distance from the coastline (km),  $D_{\text{shelf}}$  represents the average unconsolidated sediment thickness at the coastline (km),  $L_{\text{coast}}$  is the coastal length (km) of each coastal type within the COSCAT region and is then matched with the corresponding ARP’s mean fresh groundwater fraction ( $\text{FGF}_{\text{mean}}$ ) to translate the cross-sectional estimates into a 3D volume (km<sup>3</sup>), with  $p$  a constant porosity of 0.3 (–). The constant porosity value is based on several previous studies (Groen *et al* 2000, Oude Essink 2001, van Camp *et al* 2014, Zamrsky *et al* 2020). The final OFG volumes per COSCAT region presented in this study are the sum of all ARPs located within the COSCAT region. The shallow OFG volume is estimated as all fresh groundwater located offshore and above 300 meters below sea level (m bsl) (see SI figure 9), chosen arbitrarily as a depth when economically viable groundwater pumping is feasible (i.e. the infrastructure costs are lower than the value of extracted fresh water). Equation (1) is repeated by using  $\text{FGF}_{\text{min}}$  and  $\text{FGF}_{\text{max}}$  from the 24 groundwater models of each ARP to obtain uncertainty ranges per COSCAT region as well as for the global total OFG volume. The uncertainty of the latter is inflated because it assumes that geological uncertainties between COSCAT regions are fully correlated.

Potentially, brackish offshore groundwater could also be regarded as potential future water resource (Post *et al* 2013, Alsarayreh *et al* 2021, Arico *et al* 2021). That is why, additionally, the volumes of brackish offshore groundwater were also estimated using equation (1) above with OFG fraction representing volume of groundwater with concentrations lower than 10 TDS g l<sup>-1</sup>. The OFG is then subtracted from the calculated brackish offshore groundwater so only groundwater with concentrations between 1 and 10 TDS g l<sup>-1</sup> is taken into account as brackish. These brackish offshore groundwater volumes are shown in SI figure 10.

We also estimated OFG renewal time scales by fresh groundwater inflow from the landwards direction through calculating a coastal fresh groundwater discharge flux by summing up the lateral seaward flux in cells with fresh groundwater concentration at the coastline location. Since our SEAWAT models are 2D representations of the coastal groundwater flow conditions, the resulting coastal fresh groundwater discharge flux values are multiplied by the coastal length and the average unconsolidated sediment thickness at the coastline for each COSCAT region to estimate the total coastal fresh groundwater discharge flux (km<sup>3</sup> yr<sup>-1</sup>) for given coastal region. The average renewal time for a given COSCAT region is then calculated as OFG volume divided by the total coastal fresh groundwater discharge flux based on the definition of Margat and van der Gun (2013). This yields the estimated time it would take to fill the estimated OFG volume under current groundwater flow conditions. Groundwater systems with renewal times larger than 1000 years are considered non-renewable (Margat and van der Gun 2013).

### 2.3. Regional water demand and onshore groundwater extractions

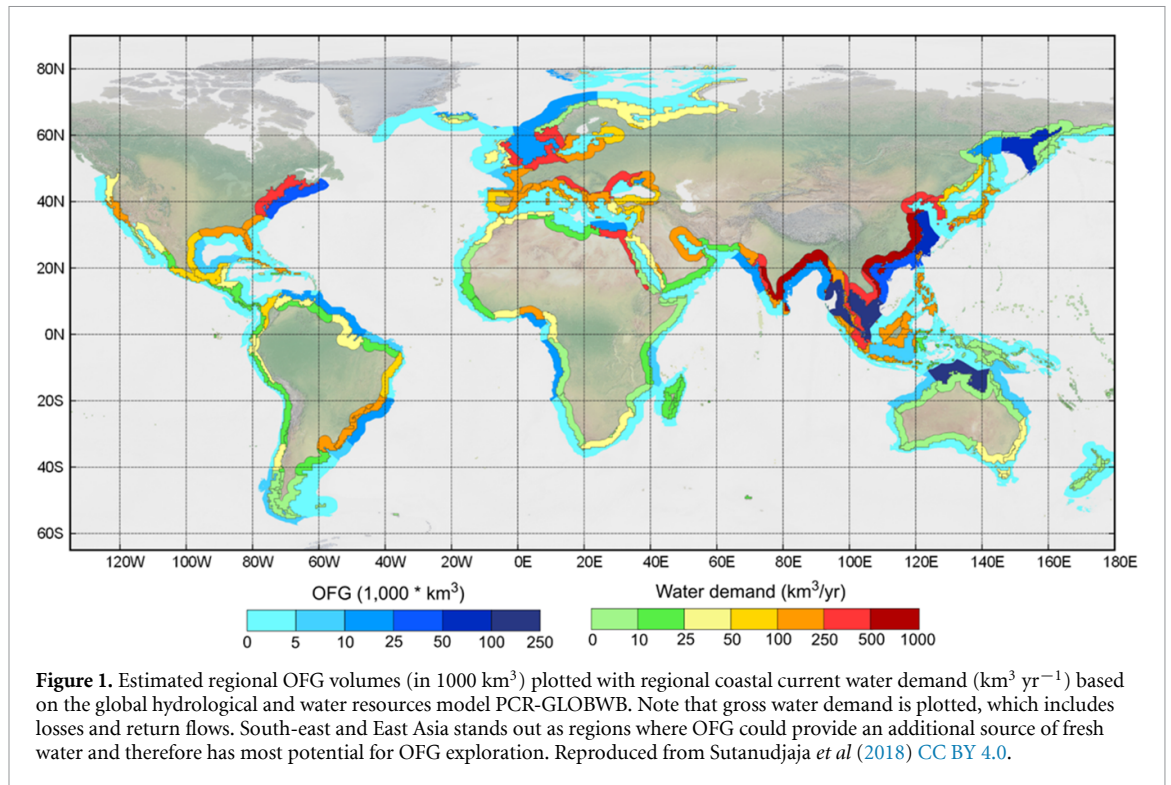
To assess the value of the estimated volumes of OFG as a potential water source for coastal water use, we compared OFG volume with regional onshore water demand and groundwater extractions estimated with the global hydrological model PCR-GLOBWB (Sutanudjaja *et al* 2018). To calculate the regional coastal water demand and groundwater extractions, we created a buffer reaching 200 km inland for each COSCAT region. The resulting buffer zones were then overlaid over the 5 arcmin PCR-GLOBWB raster output files. In such way, we were able to extract the four components of the total sectoral water demand, namely domestic, livestock, industrial and irrigation water demands. To account for climate variation and dry/wet years we averaged over 30 year time-spans to create three water demand time slices, 2020 (2005–2035), 2050 (2035–2065) and 2075 (2060–2090). The future domestic, industry and livestock water demand estimations are based on the SSP2 scenario (Kriegler *et al* 2014). To take into account the effects of climate change on the irrigation water demand, we forced

PCR-GLOBWB with the outputs of five global climate models from the RCP 6.0 climate change scenario of CMIP5, selected and bias-corrected under the ISIMIP program (Hempel *et al* 2013). The resulting future irrigation water demand is then calculated as median value of all the resulting global climate model runs. Future regional water demands together with estimated OFG volumes are shown in SI figure 6.

## 3. Results

Summing up all regional OFG volume estimates we approximate the global OFG volume to be  $1.06 \pm 0.2 \times 10^6$  km<sup>3</sup> ( $\leq 1$  g l<sup>-1</sup> TDS). However, since our groundwater models have a constant porosity value (0.3), we assess the porosity value effect on estimated OFG volume by carrying out a groundwater sensitivity study with varying porosity value (0.1, 0.2, 0.4) in a randomly selected region. We can confirm that our groundwater models with the lowest porosity (0.1) show less than half OFG fractions than the case with porosity of 0.3 (see SI figure 4). This suggests that the estimated uncertainty about the global OFG volume may be underestimated due to constant porosity considered. With that in mind, our estimated global OFG volume amounts to about 5%–10% of total fresh groundwater worldwide (estimated to be between  $10.5 \times 10^6$  km<sup>3</sup> (Gleeson *et al* 2016) and  $21.8 \times 10^6$  km<sup>3</sup> (Ferguson *et al* 2021)) and roughly 3% of total global fresh water (Shiklomanov 1998). The OFG volumes are most likely non-renewable as they were deposited during glacial periods when sea levels were substantially lower compared to current sea level. Indeed, when we calculate renewal times by the ratio of OFG volume and total coastal fresh groundwater discharge from the groundwater models (SI figure 11), we see that renewal rates exceed 1000 years for most of the coastal regions, rendering the OFG volumes effectively non-renewable.

The estimated OFG volumes vary considerably between the world's coastal regions (figure 1). Regions such as North-east USA, North Australia and South-east Asia accommodate substantial OFG volumes. However, due to unknown heterogeneity in geology and other hydrological factors (e.g. groundwater recharge, influence of rivers), the uncertainties in OFG volumes can be considerable for certain regions, e.g. the coasts around Arabian Peninsula, the Gulf Coast and the North Sea basin (SI figure 5). To put these OFG volume estimates into perspective, we compared them with extracted present day total water demand per year from simulations with a global hydrology and water resources model (Sutanudjaja *et al* 2018) for a 200 km inland buffer in each coastal region. South and South-east Asia stand out as regions with high current water demand and large OFG volumes, which calls for further investigations into more accurate quantification and potential exploration of these volumes. Water demand



is projected to increase steadily during 21st century due to population growth and climate change (Prudhomme *et al* 2014, Wada and Bierkens 2014), and OFG could prove a vital additional fresh water source in regions such as West Africa and East South America as well (SI figure 6).

We compared our OFG estimates with several regional scale studies (Oteri 1988, Groen *et al* 2000, Person *et al* 2003, 2012, Varma and Michael 2011, Zhang *et al* 2011, Bakari *et al* 2012, Amir *et al* 2013, Geldern *et al* 2013, Pauw *et al* 2014, Jiao *et al* 2015, Larsen *et al* 2017, Haroon *et al* 2018, Paleologos *et al* 2018, Engelen *et al* 2019, Gustafson *et al* 2019, Knight *et al* 2019, Thomas *et al* 2019, Bertoni *et al* 2020) and a set of offshore observation wells (Micallef 2020) limited to areas with unconsolidated sediments. Unfortunately, the majority of these regional scale studies do not provide volume estimates. Therefore, OFG's distance from coastline and depth below sea level were used as proxies. Several studies only provide one of the two proxies, while few only show OFG observations without measurements (see figure 2(A)). Fifteen regional studies covering all continents are taken into account, most of which contain both depth and distance from coast information. Our estimates are in the same order of magnitude as the observed values (figure 2(B)), with only few areas showing large discrepancies. This mostly concerns estimated thickness of OFG where our study shows thinner OFG bodies offshore as compared to literature sources. The offshore observation well dataset (Micallef 2020) gives a point measurement at a certain offshore distance and also the observed top and bottom OFG elevation.

The OFG extent is then extracted from the corresponding groundwater model of the same region at the same offshore distance as each observation well (figure 2(C)). While in the same order of magnitude, in several cases we observe a rather large difference (hundreds up to few thousands of meters) in estimated and observed OFG depth (wells ID 16, 20, 22, 23, 24, 27, 34). However, for 80% of the well locations our estimated OFG depth extents overlap the observed OFG depth ranges.

#### 4. Discussion and conclusion

Our global OFG volume estimate is in line with a previous global OFG assessment (Post *et al* 2013), which considers a more generous fresh water threshold (<10 g l<sup>-1</sup> TDS) and estimated global OFG volume along passive continental margins to be  $0.3 \times 10^6$  km<sup>3</sup>. However, this value may vary up to factor of two (Post *et al* 2013) due to uncertainty about porosity values ranging between 0.03–0.4, and explains our higher estimate which is based on a constant porosity of 0.3. Recent study by Micallef *et al* (2021) provides an estimate of offshore freshened groundwater with higher salinity (<10 g l<sup>-1</sup> TDS) than considered in our study (<1 g l<sup>-1</sup> TDS). Our modelling results show a total volume of groundwater with salinity below 10 g l<sup>-1</sup> TDS to be  $1.24 \pm 0.19 \times 10^6$  km<sup>3</sup>, which is approximately 6 times higher than the estimate by Micallef *et al* (2021) ( $0.2 \times 10^6$  km<sup>3</sup>). However, Micallef *et al* (2021) note that the actual volume of offshore freshened groundwater (and therefore also the OFG

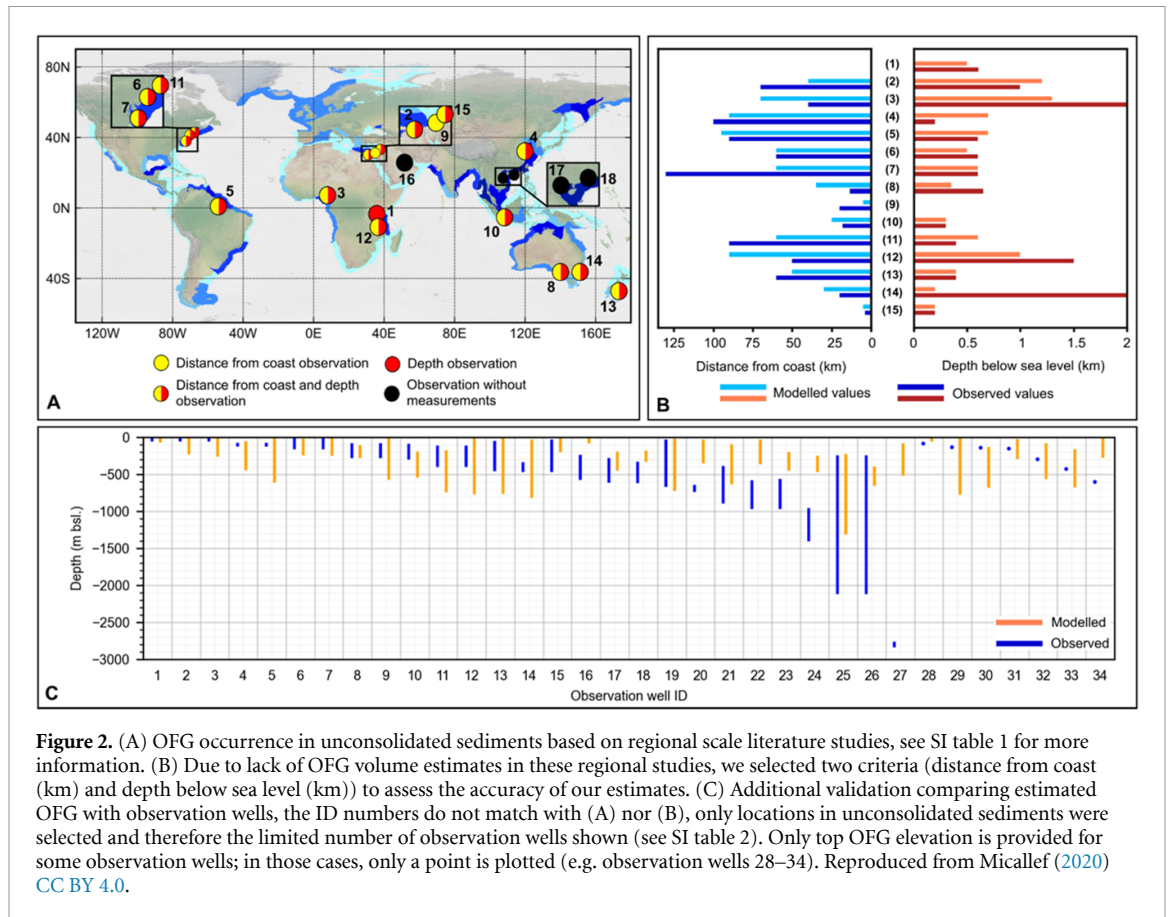
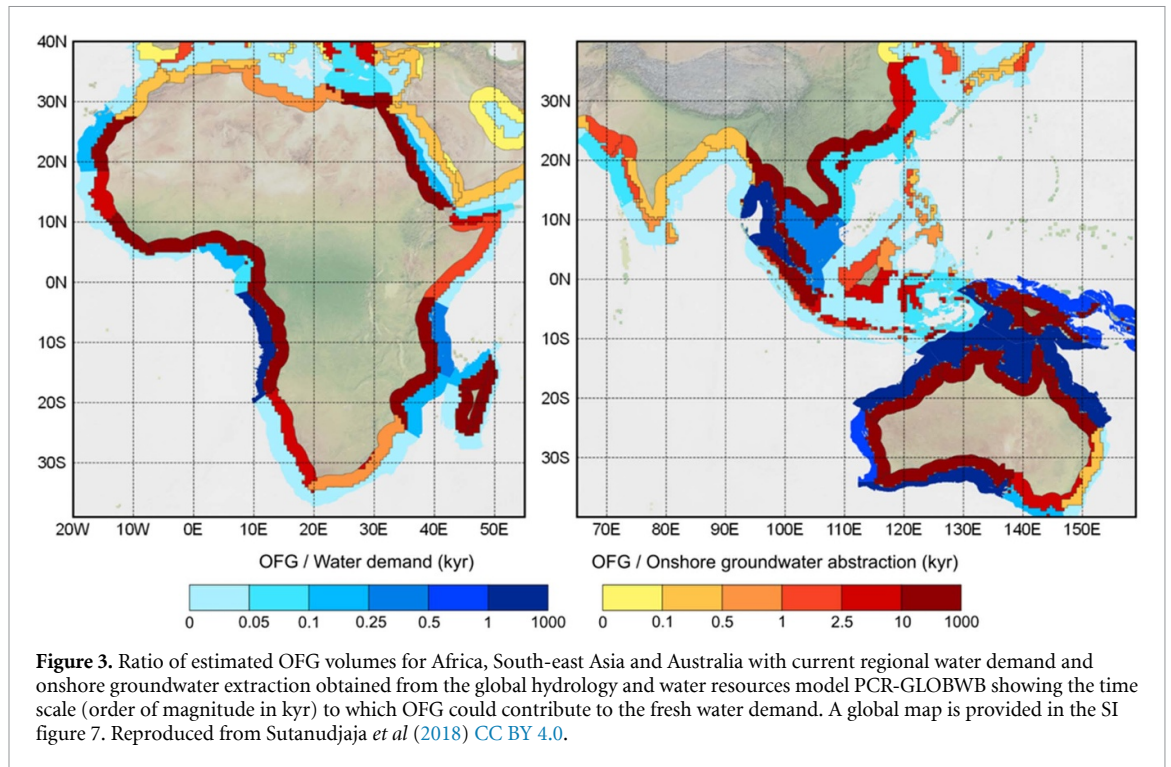


**Figure 2.** (A) OFG occurrence in unconsolidated sediments based on regional scale literature studies, see SI table 1 for more information. (B) Due to lack of OFG volume estimates in these regional studies, we selected two criteria (distance from coast (km) and depth below sea level (km)) to assess the accuracy of our estimates. (C) Additional validation comparing estimated OFG with observation wells, the ID numbers do not match with (A) nor (B), only locations in unconsolidated sediments were selected and therefore the limited number of observation wells shown (see SI table 2). Only top OFG elevation is provided for some observation wells; in those cases, only a point is plotted (e.g. observation wells 28–34). Reproduced from Micallef (2020) CC BY 4.0.

volume) is very likely higher than their estimate due to their methodology only considering offshore groundwater emplaced by meteoric recharge and their measurement database often does not provide the full extent of the offshore freshened groundwater bodies. This suggests that our study possibly overestimates the OFG volume along the global coastline but nevertheless provides an estimate in the same order of magnitude as previous global studies (based mostly on qualitative analyses). This can be partly explained by simplifications made during our groundwater modelling study (24 geological scenarios per coastal region) and subsequent OFG volume calculation for each coastal region, where we assume a single cross-sectional groundwater salinity distribution over lengthy coastline stretches. Comparing regional cross-sectional OFG schematizations with our groundwater model results shows a relatively good match in terms of OFG extent and depth (figure 2(B)), but we can also observe some discrepancies presumably due to the large-scale nature of our analysis. As expected, this scale discrepancy is more pronounced when comparing top and bottom of OFG estimates with local observation wells (figure 2(C)). Furthermore, since in our study we only consider unconsolidated sediment systems, older unconsolidated sediment aquifers overlaid by rock formations (e.g. sandstone, limestone) are not accounted for in our approach. This can lead to

missing OFG reserves in the deeper formations by our groundwater models as is the case for the Gippsland basin in South Australia (Varma and Michael 2011) (see figure 2(C), observation well 27). Other reasons for larger discrepancies can be caused by the scale difference between local point measurements and our average OFG estimates for regions spanning over hundreds (up to thousands) of kilometers of coastline. It is also possible that the individual observation well measurements were only conducted at a certain depth and do not provide the full extent of the actual range of OFG extent at a given location. Despite this, a satisfactory match is observed in shallower unconsolidated sediment depths (up to 500 m bsl.) which suggests that our approach can be used to estimate regional OFG volumes.

While our offshore fresh (or freshened) groundwater volume estimates are accordance with previous studies, there are a number of limitations and uncertainties that have to be addressed. First, the extent of the cross-sectional profiles is limited to up to 200 km offshore. The majority of the offshore freshened groundwater occurrences have been reported to lie within 55 km distance from the current coastline but the maximum distance has been reported to be 720 km (Micallef *et al* 2021). This means that in some areas our cross-sectional profiles possibly do not capture the full extent of OFG bodies. Our OFG volume calculations use a regional coastal



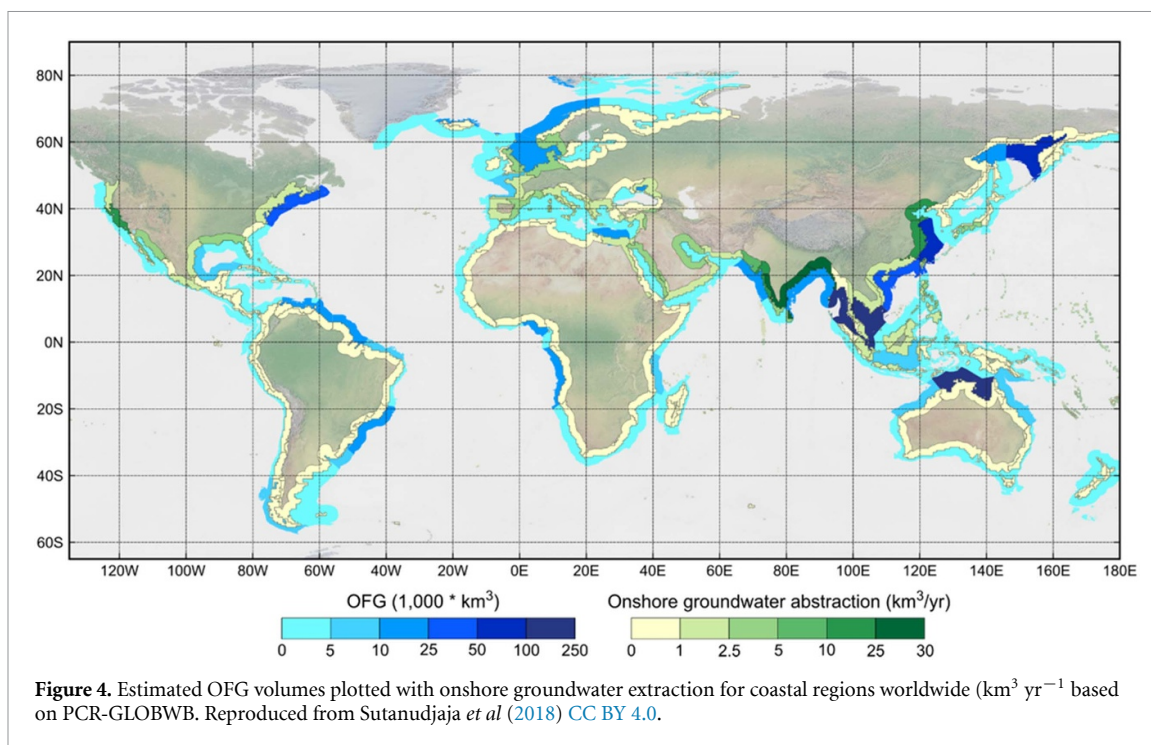
length neglecting local and regional curvature. This simplification can lead to OFG volume overestimates as coastline curvatures (e.g. bay and lagoon areas) are not taken into account leading to artificially stretching the coastal length in our calculation. The constant porosity of 0.3 that is used in the groundwater models contributes to underestimating the uncertainty in the global OFG volume. We can deduce that from the sensitivity study with varying porosity values (see SI figure 4 and SI table 3) that shows non-linear decline in estimated OFG volume with lower porosity values. On average, the groundwater models with the lowest porosity value (0.1) show a lower estimated OFG by 11%. This means that the estimated global OFG volume would be lower by  $0.11 \times 10^6 \text{ km}^3$  than estimated by groundwater models with the constant porosity value equal to 0.3. The differences in estimated mean fresh groundwater fraction between the simulations with low porosity (0.1) and the constant porosity value considered in this study (0.3) can vary from 0.4% up to 34.5% (see SI table 3). Therefore, it is important to take this into account when conducting regional scale studies to investigate the potential impact of varying porosity on the OFG conditions in a given region.

Comparing the estimated OFG volume with current regional water demand highlights areas where OFG exploration could provide a sustainable fresh water source over long periods of time (up to millennia). South-east Asia, West Africa and most of Australia show the highest potential for OFG exploration (figures 3 and 4; SI figures 7 and 8). Exploring OFG as potential fresh water source could be especially interesting in densely populated and intensely

farmed deltaic areas (SI table 4). However, more detailed regional hydrogeological and economic analyses are necessary to identify the exact potential the OFG brings to regional usage as source of fresh water. OFG volumes found in several regions could provide multiple centuries (even up to two millennia) worth of fresh groundwater under current and under future water demand rates. However, salinization of inland aquifers might occur when extracting these OFG volumes and this process should be further studied before extracting OFG. This threat is examined by previous studies showing that extracting OFG as an additional source of fresh water for coastal communities is deemed to have potential impacts (Knight *et al* 2018) on environmental and human conditions while its feasibility should be evaluated for each site (Haakon and Fridtjof 2012).

We also evaluated total OFG volume at shallow depths (higher than 300 m below average sea level; SI figure 9). We estimate the total volume of shallow OFG to be approximately 30% of total OFG volume ( $\sim 0.31 \times 10^6 \text{ km}^3$ ), showing still substantial shallow OFG volumes in e.g. South and South-east Asia. The shallow depths are of interest because pumping from deeper formations is more expensive and has a higher potential to disturb onshore groundwater heads (Yu and Michael 2019) in regions where onshore and offshore aquifer layers are interconnected. The connection of the onshore and offshore aquifers is shown to lead to larger OFG volumes via preferential pathways in heterogeneous geological systems as compared to homogeneous systems (Michael *et al* 2016, Knight *et al* 2018). Our geological scenarios take into account geological heterogeneity





and simulate onshore and offshore interconnectivity (see SI figure 2). However, more local and regional geological information (e.g. boreholes, faults, geological models) is necessary to improve regional scale simulation of OFG.

To conclude, our analysis shows that there are potentially large OFG volumes of up to 10% of total fresh terrestrial groundwater deposited in unconsolidated sediment systems in many regions worldwide. Exploring these offshore resources could provide additional fresh water sources for agricultural, industrial or domestic use. In South-east and East Asia, West Africa and several regions in South America. OFG could prove to be a vital water stress mitigating factor, especially in regions facing near future increases in water demand due to population growth and climate change throughout the 21st century. Further research should investigate the effects of offshore pumping on groundwater levels inland as those could be interlinked. The OFG extraction can potentially lead to onshore groundwater level drops even in shallower aquifers (Yu and Michael 2019) which could have negative impact environmental conditions and societal fresh water needs. Moreover, searching for new hydrogeological data sources, implementing these in local to regional scale hydrogeological modelling studies would help to better understand the extent and behaviour of these offshore fresh (and brackish) groundwater reserves.

### Data availability statement

The data that support the findings of this study are openly available at the following URL/DOI:

[10.5281/zenodo.3937204](https://doi.org/10.5281/zenodo.3937204). The final groundwater salinity estimations for each COSCAT region (as 2D profiles) are provided there as well as shapefiles containing offshore fresh (and brackish) groundwater volumes together with inland water demand and groundwater extraction rates.

### Acknowledgments

This study's calculations were performed on the Dutch national supercomputer Cartesius with the support of SURE. This research was funded by the Netherlands Organization for Scientific Research (NWO) under the STW project 'Water Nexus: Resource Analysis and Regional Water Management' (No. 14298).

### Author contributions

D Z, M F P B and G H P O E designed the study and wrote the manuscript. D Z performed the model calculations and data analysis. E H S and L P H (R) v B provided coastal water demand data and helped improve the manuscript.

### ORCID iDs

Daniel Zamrsky  <https://orcid.org/0000-0001-6046-688X>

Gualbert H P Oude Essink  <https://orcid.org/0000-0003-0931-6944>

Marc F P Bierkens  <https://orcid.org/0000-0002-7411-6562>

## References

- Alsarayreh A A, Al-Obaidi M A, Farag S K, Patel R and Mujtaba I M 2021 Performance evaluation of a medium-scale industrial reverse osmosis brackish water desalination plant with different brands of membranes. A simulation study *Desalination* **503** 114927
- Amir N, Kafri U, Herut B and Shalev E 2013 Numerical simulation of submarine groundwater flow in the coastal aquifer at the Palmahim area, the Mediterranean Coast of Israel *Water Res. Manage.* **27** 4005–20
- Arico Q L, Kassis Z R, Maliva R G, Weixing Guo W, Manahan S and Missimer T M 2021 Changes in pumping-induced groundwater quality used to supply a large-capacity brackish-water desalination facility, Collier County, Florida: a new aquifer conceptual model *Water* **13** 1951
- Bakari S S, Aagaard P, Vogt R D, Ruden F, Brennwald M S, Johansen I and Gulliksen S 2012 Groundwater residence time and paleorecharge conditions in the deep confined aquifers of the coastal watershed, South-East Tanzania *J. Hydrol.* **466–467** 127–40
- Bertoni C, Lofi J, Micallef A and Moe H 2020 Seismic reflection methods in offshore groundwater research *Geosciences* **10** 1–34
- Chen Z et al 2017 The World Karst Aquifer Mapping project: concept, mapping procedure and map of Europe *Hydrogeol. J.* **25** 771–85
- Engelen J V, Verkaik J, King J, Nofal E R, Bierkens M F P and Oude Essink G H 2019 A three-dimensional palaeohydrogeological reconstruction of the groundwater salinity distribution in the Nile Delta Aquifer *Hydrol. Earth Syst. Sci.* **2014** 5175–98
- Fan Y, Li H and Miguez-Macho G 2013 Global patterns of groundwater table depth *Science* **339** 940–3
- Faneca Sánchez M, Gunnink J L, van Baaren E S, Oude Essink G H P, Siemon B, Auker E, Elderhorst W and de Louw P G B 2012 Modelling climate change effects on a Dutch coastal groundwater system using airborne electromagnetic measurements *Hydrol. Earth Syst. Sci.* **16** 4499–516
- Ferguson G et al 2021 Crustal groundwater volumes greater than previously thought *Geophys. Res. Lett.* **48** e2021GL093549
- Geldern R V, Hayashi T, Böttcher M E, Mottl M J, Barth J A C and Stadler S 2013 Stable isotope geochemistry of pore waters and marine sediments from the New Jersey shelf: methane formation and fluid origin *Geosphere* **9** 96–112
- Giosan L, Syvitski J, Constantinescu S and Day J 2014 Protect the world's deltas *Nature* **516** 31–33
- Gleeson T, Befus K M, Jasechko S, Luijendijk E and Cardenas M B 2016 The global volume and distribution of modern groundwater *Nat. Geosci.* **9** 161–4
- Gleeson T, Moosdorf N, Hartmann J and van Beek L P H 2014 A glimpse beneath earth's surface: global hydrogeology maps (GLHYMPS) of permeability and porosity *Geophys. Res. Lett.* **41** 3891–8
- Grant K M, Rohling E J, Bar-Matthews M, Ayalon A, Medina-Elizalde M, Ramsey C B, Satow C and Roberts A P 2012 Rapid coupling between ice volume and polar temperature over the past 150,000 years *Nature* **491** 744–7
- Groen J, Velstra J and Meesters A G C A 2000 Salinization processes in paleowaters in coastal sediments of Suriname: evidence from  $\delta^{37}\text{Cl}$  analysis and diffusion modelling *J. Hydrol.* **234** 1–20
- Gustafson C, Key K and Evans R L 2019 Aquifer systems extending far offshore on the U.S. Atlantic margin *Sci. Rep.* **9** 1–10
- Haakon T and Fridtjof B 2012 Submarine groundwater: a new concept for the supply of drinking water *Water Resour. Manage.* **26** 1015–26
- Haroon A, Lippert K, Mogilatov V and Tezkan B 2018 First application of the marine differential electric dipole for groundwater investigations: a case study from Bat Yam, Israel *Geophysics* **83** B59–B76
- Hartmann J and Moosdorf N 2012 The new global lithological map database GLiM: a representation of rock properties at the Earth surface *Geochem. Geophys. Geosyst.* **13** 1–37
- Hathaway J C, Poag C W, Valentine P C, Manheim F T, Kohout F A, Bothner M H, Miller R E, Schultz D M and Sangrey D A 1979 U.S. geological survey core drilling on the Atlantic shelf *Science* **206** 515–27
- Head M J and Gibbard P L 2005 *Early–Middle Pleistocene Transitions: The Land–Ocean Evidence* (London: Geological Society of London) (<https://doi.org/10.1144/GSL.SP.2005.247>)
- Hempel S, Frieler K, Warszawski L, Schewe J and Piontek F 2013 A trend-preserving bias correction—the ISI-MIP approach *Earth Syst. Dyn.* **4** 219–36
- Hengl T et al 2014 SoilGrids1km—global soil information based on automated mapping *PLoS One* **9** e105992
- Huscroft J, Gleeson T, Hartmann J and Börker J 2018 Compiling and mapping global permeability of the unconsolidated and consolidated earth: global hydrogeology maps 2.0 (GLHYMPS 2.0) *Geophys. Res. Lett.* **45** 1897–904
- Jiao J J, Shi L and Kuang X 2015 Reconstructed chloride concentration profiles below the seabed in Hong Kong (China) and their implications for offshore groundwater resources *Hydrogeology Journal* **23** 277–86
- Knight A C, Werner A D and Irvine D J 2019 Combined geophysical and analytical methods to estimate offshore freshwater extent *J. Hydrol.* **576** 529–40
- Knight A C, Werner A D and Morgan L K 2018 The onshore influence of offshore fresh groundwater *J. Hydrol.* **561** 724–36
- Kriegler E, Edmonds J, Hallegatte S, Ebi K L, Kram T, Riahi K, Winkler H and van Vuuren D P 2014 A new scenario framework for climate change research: the concept of shared climate policy assumptions *Clim. Change* **122** 401–14
- Lambeck K, Rouby H, Purcell A, Sun Y and Sambridge M 2014 Sea level and global ice volumes from the last glacial maximum to the holocene *Proc. Natl Acad. Sci.* **111** 15296–303
- Langevin C D and Guo W 2006 MODFLOW/MT3DMS-based simulation of variable-density groundwater flow and transport *Ground Water* **44** 339–51
- Larsen F, Tran L V, Hoang H V, Tran L T, Christiansen A V and Pham N Q 2017 Groundwater salinity influenced by holocene seawater trapped in incised valleys in the Red River delta plain *Nat. Geosci.* **10** 376–81
- Laruelle G G, Dürr H H, Lauerwald R, Hartmann J, Slomp C P, Goossens N and Regnier P A G 2013 Global multi-scale segmentation of continental and coastal waters from the watersheds to the continental margins *Hydrol. Earth Syst. Sci.* **17** 2029–51
- Levi E, Goldman M, Tibor G and Herut B 2018 Delineation of subsea freshwater extension by marine geoelectromagnetic soundings (SE Mediterranean Sea) *Water Resour. Manage.* **32** 3765–79
- Margat J and van der Gun J 2013 *Groundwater around the World: A Geographic Synopsis* (Boca Raton, FL: Taylor & Francis Group, LLC) ISBN:978-0-203-77214-0
- Meisler H, Leahy P P and Knobel L L 1984 Effect of eustatic sea-level changes on saltwater-freshwater in the Northern Atlantic Coastal Plain *USGS Water Supply Paper: 2255* (available at: <https://pubs.er.usgs.gov/publication/wsp2255> (accessed 6 December 2021))
- Meybeck M, Dürr H H and Vörösmarty C J 2006 Global coastal segmentation and its river catchment contributors: a new look at land-ocean linkage *Glob. Biogeochem. Cycles* **20** 1–15
- Micallef A et al 2020 3D characterisation and quantification of an offshore freshened groundwater system in the Canterbury Bight *Nat. Commun.* **11** 1372
- Micallef A 2020 Global database of offshore freshened groundwater records (<https://doi.org/10.5281/ZENODO.4247833>)
- Micallef A et al 2021 Offshore freshened groundwater in continental margins *Rev. Geophys.* **59** e2020RG000706

- Michael H A, Scott K C, Koneshloo M, Yu X, Khan M R and Li K 2016 Geologic influence on groundwater salinity drives large seawater circulation through the continental shelf *Geophys. Res. Lett.* **43** 10,782–10,791
- Minderhoud P S J, Erkens G, Pham V H, Bui V T, Erban L, Kooi H and Stouthamer E 2017 Impacts of 25 years of groundwater extraction on subsidence in the Mekong delta, Vietnam *Environ. Res. Lett.* **12** 064006
- Montzka C, Herbst M, Weihermüller L, Verhoef A and Vereecken H 2017 A global data set of soil hydraulic properties and sub-grid variability of soil water retention and hydraulic conductivity curves *Earth Syst. Sci. Data Discuss.* **9** 1–25
- Morgan L K, Werner A D and Patterson A E 2018 A conceptual study of offshore fresh groundwater behaviour in the Perth Basin (Australia): modern salinity trends in a prehistoric context *J. Hydrol. Reg. Stud.* **19** 318–34
- NTSG 2019 MODIS global evapotranspiration project (MOD16) (available at: [www.ntsg.umt.edu/project/modis/mod16.php](http://www.ntsg.umt.edu/project/modis/mod16.php)) (Accessed 24 July 2019)
- Oteri A U 1988 Electric log interpretation for the evaluation of salt water intrusion in the eastern Niger Delta *Hydrol. Sci. J.* **33** 19–30
- Oude Essink G H P 2001 Saltwater intrusion in 3D large-scale aquifers: a Dutch case *Phys. Chem. Earth B* **26** 337–44
- Oude Essink G H P, Baaren E S V and Louw P G B D 2010 Effects of climate change on coastal groundwater systems: a modeling study in the Netherlands *Water Resour. Res.* **46** 1–16
- Paleologos E K, Farouk S and Nahyan M T A 2018 Water resource management towards a sustainable water budget in the United Arab Emirates *IOP Conf. Ser.: Earth Environ. Sci.* **191** 012007
- Pauw P S, van der Zee S E A T M, Leijnse A, Delsman J R, De Louw P G B, De Lange W J and Oude Essink G H P 2014 Low-resolution modeling of dense drainage networks in confining layers *Ground Water* **5** 1–11
- Person M et al 2003 Pleistocene hydrogeology of the Atlantic continental shelf, New England *GSA Bulletin* **115** 1324–43
- Person M, Marksamer A, Dugan B, Sauer P E, Brown K, Bish D, Licht K J and Willett M 2012 Use of a vertical  $\delta^{18}\text{O}$  profile to constrain hydraulic properties and recharge rates across a glacio-lacustrine unit, Nantucket Island *Hydrogeol. J.* **20** 325–36
- Post V E A, Groen J, Kooi H, Person M, Ge S and Edmunds W M 2013 Offshore fresh groundwater reserves as a global phenomenon *Nature* **504** 71–78
- Prudhomme C et al 2014 Hydrological droughts in the 21st century, hotspots and uncertainties from a global multimodel ensemble experiment *Proc. Natl Acad. Sci. USA* **111** 3262–7
- Rasmussen P, Sonnenborg T O, Gonciar G and Hinsby K 2013 Assessing impacts of climate change, sea level rise, and drainage canals on saltwater intrusion to coastal aquifer *Hydrol. Earth Syst. Sci.* **17** 421–43
- Shiklomanov I A 1998 *World Water Resources, A New Appraisal and Assessment for the 21st Century* (Paris: UNESCO) (<https://snia.mop.gov.cl/sad/PHI710.pdf>)
- Sutanudjaja E H et al 2018 PCR-GLOBWB 2: a 5 arcmin global hydrological and water resources model *Geosci. Model Dev.* **08** 2429–53
- Syvitski J P M et al 2009 Sinking deltas due to human activities *Nat. Geosci.* **2** 681–6
- Tessler Z D, Vörösmarty C J, Grossberg M, Gladkova I, Aizenman H, Syvitski J P M and Foufoula-Georgiou E 2015 Profiling risk and sustainability in coastal deltas of the world *Science* **349** 638–43
- Thomas A T, Reiche S, Riedel M and Clauser C 2019 The fate of submarine fresh groundwater reservoirs at the New Jersey shelf, USA *Hydrogeol. J.* **27** 2673–94
- van Camp M, Mtoni Y, Mjemah I C, Bakundukize C and Walraevens K 2014 Investigating seawater intrusion due to groundwater pumping with schematic model simulations: the example of the Dar es Salaam coastal aquifer in Tanzania *J. Afr. Earth Sci.* **96** 71–78
- Varma S and Michael K 2011 Impact of multi-purpose aquifer utilisation on a variable-density groundwater flow system in the Gippsland Basin, Australia *Hydrogeol. J.* **20** 119–34
- Wada Y and Bierkens M F P 2014 Sustainability of global water use: past reconstruction and future projections *Environ. Res. Lett.* **9** 104003
- Weatherall P, Marks K M, Jakobsson M, Schmitt T, Tani S, Arndt J E, Rovere M, Chayes D, Ferrini V and Wigley R 2015 A new digital bathymetric model of the world's oceans *Earth Space Sci.* **2** 331–45
- World Health Organization 2017 *Guidelines for Drinking-water Quality: Fourth Edition Incorporating the First Addendum* (World Health Organization) 631 ISBN-978-92-4-154995-0
- Wu Z, Li J, Li S, Shang J and Jin X 2017 A new method to identify the foot of continental slope based on an integrated profile analysis *Mar. Geophys. Res.* **38** 199–207
- Yamanaka T, Shimada J, Tsujimura M, Lorphensri O, Mikita M, Hagihara A and Onodera S 2011 Tracing a confined groundwater flow system under the pressure of excessive groundwater use in the lower central plain, Thailand *Hydrol. Process.* **25** 2654–64
- Yang J, Zhang H, Yu X, Graf T and Michael H A 2018 Impact of hydrogeological factors on groundwater salinization due to ocean-surge inundation *Adv. Water Resour.* **111** 423–34
- Yu X and Michael H A 2019 Offshore pumping impacts onshore groundwater resources and land subsidence geophysical research letters *Geophys. Res. Lett.* **46** 2553–62
- Yu X, Yang J, Graf T, Koneshloo M, O'Neal M A and Michael H A 2016 Impact of topography on groundwater salinization due to ocean surge inundation *Water Resour. Res.* **52** 5794–812
- Zamrsky D, Karssenberg M E, Cohen K M, Bierkens M F P and Oude Essink G H P 2020 Geological heterogeneity of coastal unconsolidated groundwater systems worldwide and its influence on offshore fresh groundwater occurrence *Front. Earth Sci.* **7** 1–23
- Zamrsky D, Oude Essink G H P and Bierkens M F P 2018 Estimating the thickness of unconsolidated coastal aquifers along the global coastline *Earth Syst. Sci. Data* **10** 1–19
- Zhang Z, Zou L, Cui R and Wang L 2011 Study of the storage conditions of submarine freshwater resources and the submarine freshwater resources at north of Zhoushan sea area *Mar. Sci. Bull.* **30** 47–52 ISSN: 1001-6392